International Journal of Engineering, Mathematical and Physical Sciences
ISSN: 2517-9934
Vol:7, No:6, 2013

A Numerical Simulation of the Indoor Air Flow

Karel Fraňa, Jianshun S. Zhang and Miloš Müller

Abstract—The indoor airflow with a mixed natural/forced convection was numerically calculated using the laminar and turbulent approach. The Boussinesq approximation was considered for a simplification of the mathematical model and calculations. The results obtained, such as mean velocity fields, were successfully compared with experimental PIV flow visualizations. The effect of the distance between the cooled wall and the heat exchanger on the temperature and velocity distributions was calculated. In a room with a simple shape, the computational code OpenFOAM demonstrated an ability to numerically predict flow patterns. Furthermore, numerical techniques, boundary type conditions and the computational grid quality were examined. Calculations using the turbulence model k-omega had a significant effect on the results influencing temperature and velocity distributions.

Keywords—natural and forced convections, numerical simulations, indoor airflows.

I. Introduction

THE ventilation in a room is a powerful instrument for maintaining acceptable indoor air quality. However, in an inappropriate regime, the ventilation can cause a lot of air flow problems associated with indoor air quality e.g. a localized higher contaminant concentration can appear due to insufficient flow. In order to avoid that, simulation techniques can predict inappropriate flow conditions in advance so that the layout of the room or the geometry of a ventilation system can be changed before these rooms are occupied. Furthermore, air flow studies can reduce energy demand e.g. by a flow rate optimization.

In practice, the air flow in the room is a complex subject involving turbulence, flow separation, recirculation and the buoyancy effect. Posner et al. [7] compared results from 3D CFD with laser Doppler Anemometry (LDA) and particle Image Velocimetry (PIV) of indoor air flows. This study took into account the furniture in the room and therefore the flow problem came to be complex. Geometry details started to play a crucial role and they had a large impact on the air flow behavior. Nevertheless, the RNG k-epsilon model and laminar approach revealed the best results with relatively good correlation to experimental evidence. As an explanation, this low Reynolds number flow was not appropriate for the RNG k-epsilon turbulence model. It is because the effect of the turbulence is weak and turbulence modeling has a negligible effect on the flow behavior.

The air flow study comes to be especially complicated if a natural convection from the human body is considered in the study as well. This flow pattern was investigated experimentally and numerically in [8]. Similarly, as in the previous work, the RNG k-epsilon turbulence model was preferred for turbulence flow simulations.

Besides RANS techniques, the Large Eddy simulation approach was adopted for indoor air flow simulations with natural and forced (mixed) convection flows in rooms. The filtering technique with a dynamic subgrid scale model referred to as FDSM was successfully applied. As a result, the predicted air velocity, temperature and turbulence distributions agreed well with the corresponding experimental data [9].

Because of frequent complexities caused by wide ranging room layouts and flow conditions etc., numerous computational techniques were used for indoor air flow studies. On the whole, the reasonable numerical results demonstrated that the CFD tools are a powerful instrument for indoor air quality studies [2], [4], [7] - [10].

K. Fraňa and M. Müller are with the Department of Power Engineering Equipment, Technical University of Liberec, 461 17 Czech Republic e-mail: karel.frana@tul.cz, milos.muller@tul.cz.

Jianshun S. Zhang is Professor and Director at the Building Energy & Environmental Systems Laboratory (BEESL), Department of Mechanical and Aerospace Engineering, 263 Link Hall, Syracuse University, Syracuse, NY 13244-1240 USA e-mail: jszhang@syr.edu, http://beesl.syr.edu/

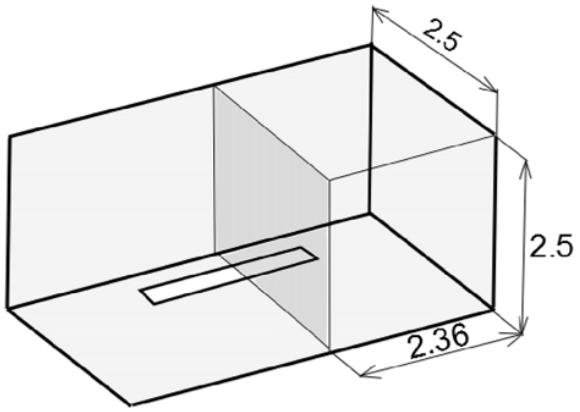

Fig. 1. Sketch of the laboratory and a depiction of the half model used as a computational domain.

II. Problem formulation

The incompressible unsteady turbulent flow with mixed convection was considered in a room heated by a floor coin. The size of the computational domain is 2,5 x 2,36 x 2,5. This size corresponds to one half of the real laboratory used for experimental measurements. Fig. 1 shows the laboratory and details of the laboratory were described in [6].

The governing equations expressing the conservation of mass, momentum and energy with the Boussinesq approximation are as follows:

$$\frac{\partial u_j}{\partial x_j} = 0 \quad (1)$$

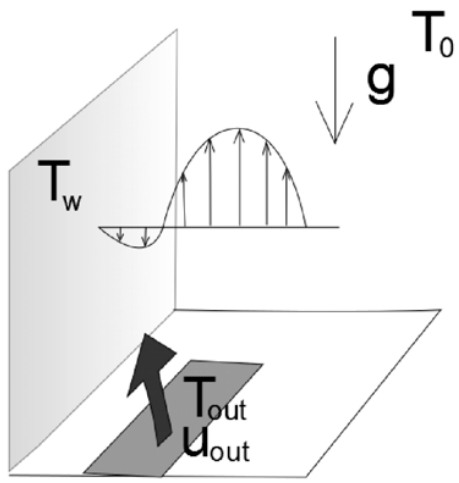

Fig. 2. Sketch of the flow problem with mixed heat convection.

$$\frac{\partial u_i}{\partial t} + \frac{\partial}{\partial x_j}\left(u_j u_i\right) = -\frac{\partial \tilde{p}}{\partial x_i} + \frac{\partial}{\partial x_j}\left[\nu_{eff}\left(\frac{\partial u_i}{\partial x_j} + \frac{\partial u_j}{\partial x_i}\right)\right] + g_i\left[1 - \beta\left(T - T_0\right)\right] \quad (2)$$

$$\frac{\partial T}{\partial t} + \frac{\partial}{\partial x_j}\left(T u_j\right) = \frac{\partial}{\partial x_k}\left(k_{eff}\frac{\partial T}{\partial x_k}\right) \quad (3)$$

where u is the average velocity field, T is average temperature and p is a modified mean pressure. The effective thermal conductivity is $k_{eff} = \nu_t/Pr_t + \nu_0/Pr$, where ν_t and ν_0 is turbulent kinematic viscosity and kinematic viscosity, respectively, and Pr_t is the turbulent Prandtl number.

The last term in Equation 2 denotes the Boussinesq approximation, where β is thermal expansion and g_i is gravity acceleration. The Boussinesq approximation is introduced to reduce the degree of the complexity of density variations and implies that density effects are considered only in the buoyancy force term of the momentum equation. This simplicity leads to restrictions as follows: Variations of all fluid properties other than the density with temperature are ignored completely. Density variations result mainly from temperature variations. The density variations are taken to have a small effect on the inertial mass of the fluid motion through the effect of gravity [1].

The study of the indoor air flow with mixed convection considers a relatively small temperature difference of 11 K. This small temperature difference has a negligible effect on the flow variables. The Boussinesq approximation introduces errors less than 1 percent for temperature variations up to 15 K for air [3] and [2]. Therefore, the BuoyancyBoussinesq solver in OpenFOAM has been used for calculations.

The relevant flow parameter of the mixed convection is a Grashof number that is defined as follows

$$Gr = \frac{\beta g\left(T_{out} - T_0\right)L^3}{\nu^2} \quad (4)$$

where T_{out} is the temperature of the flow stream, T_0 the surrounding temperature and l_{ch} is a characteristic length scale defined by the height of the computational domain. The other relevant parameter used for forced convection is the Reynolds number defined as

$$Re = \frac{u_{out} l_{ch}}{\nu} \quad (5)$$

where u_{out} is the velocity of the heated flow entering into the heated room (computational domain) and l_{ch} is a characteristic length scale defined as follows

$$l_{ch} = \frac{2lh}{(l+h)} \quad (6)$$

where l is the length of the heat floor convector and h is the width of the heat floor convector. The indoor air flow was calculated as a laminar. For purpose of the testing, the turbulence model $k - omega$ model was used for locally turbulent flow behavior. This model is based on the model [11].

III. Numerical simulation and experiments

The numerical study was carried out in the computational code OpenFOAM. The computational grid consisted of hexahedra type cells with various grid spacings. The smooth grid refinement was close to the cooling vertical walls and in the region above the heating coil. The rest of the computational domain was meshed by a relatively coarse grid spacing. Fig. 3 shows the grid spacing in the slice throughout the computational domain. The minimal cell volume in the smooth grid region was 1.64×10^{-6} and maximal cell volume was 1.53×10^{-4}, respectively. The computational grid consisted of 930,000 cells.

Fig. 4 illustrates the computational domain with prescribed boundary conditions. At the inlet or hot wall, the velocity value of 0.14 m/s with 308 K $1.03T_0$ was defined. The velocity and temperature values were measured using hot wire anemometry. The cooling wall was set up with temperature values varying from 283 K ($0.95T_0$) to 299 K (the surrounding temperature T_0). Because of the flow and geometrical symmetry, only half of the computational domain is considered and a symmetry plane was described at one boundary condition. The boundaries at the top and in the front were defined as an inletOutlet type boundary. The bottom was considered as a wall type boundary.

The flow behavior is described by the governed equations involved in the gradient derivate terms, Laplacian terms and divergence derivate terms. The gradient derivate terms were treated by a Gauss linear second-order scheme, the Laplacian terms by a Gauss linear corrected scheme (second-order conservative scheme) and the divergence terms by a Gauss limited linear second order scheme. Time discretization was carried out using the Euler method which provided a first order implicit integration. Linear equations were solved by a preconditioned conjugated gradient iteration technique.

The flow was visualized using the PIV (Particle Image Velocimetry) method [4] and [5]. Sketch of the measurement is depicted in Fig. 5 . In this method a circular laser beam is

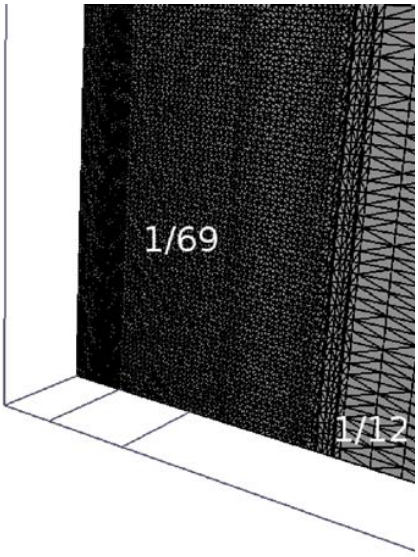

Fig. 3. Slice throughout the computational domain with the mesh size

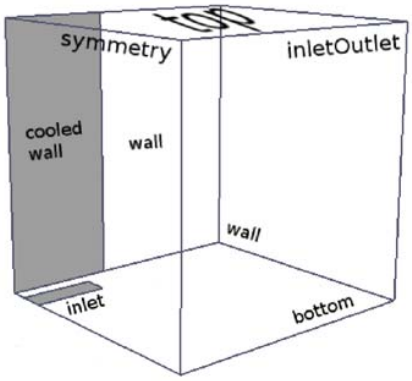

Fig. 4. Description of the boundary conditions

transformed through a spherical optic into a sheet of light. The sheet of light is focused into the region where the flow has to be visualized. The flow from the convector is saturated by a visualization fluid which is illuminated by the sheet of light. The saturation is provided by a perforated hose placed on the front edge of the convector. The flow is recorded by a PIV camera with the optical axis oriented perpendicularly to the sheet. The figures from the camera are elaborated by a cross-correlation technique in Dantec Dynamic Studio software. The results are provided in the form of a velocity field.

IV. Results

The indoor air flow in the room is controlled mainly by the inlet velocity generated in the heat exchanger located under the floor and by the cooled wall if the temperature of the cooled wall is lower than the surrounding temperature. The assumption is that the particular condition given by a maximal velocity and the lowest wall temperature, gives a ratio between the Grashof number and the square of the Reynolds number of

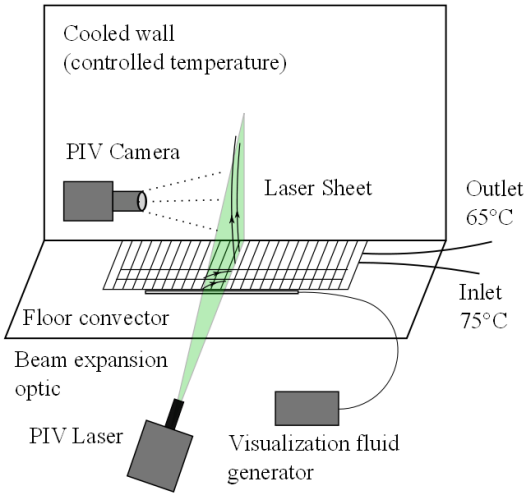

Fig. 5. Sketch of the PIV measurement of the velocity field

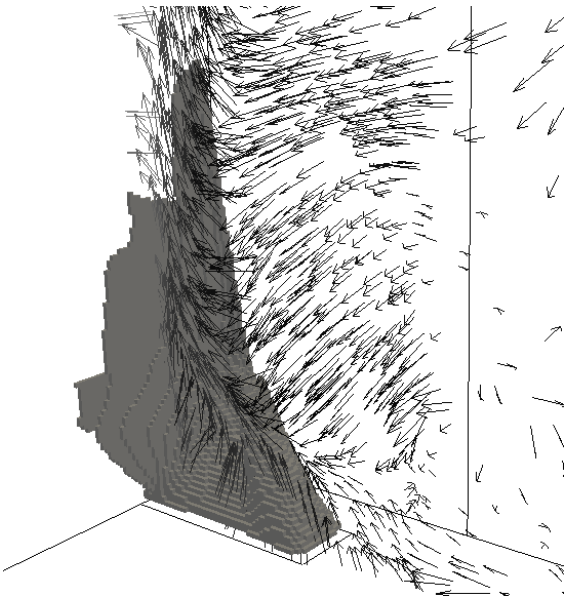

Fig. 6. The temperature isosurfaces with the mean velocity vector field

0.066. This value is much lower than one, therefore, this flow can be considered as a forced convection flow. The relevant parameter will be the Reynolds number.

Fig. 6 illustrates the iso-surfaces of the temperature representing temperature levels between 1.01 T_0 and 1.03 T_0, where T_0 is the surrounding temperature. In practice, the heated air flow with a particular velocity magnitude leaves the heat exchanger located under the floor (not visible in the figure). This air flow is afterwards shifted towards the symmetry plane of the model because of the effect of the stronger crosswise flow. The existence of the crosswise oriented flow is depicted using the mean velocity vectors in Fig. 7. Additionally, the numerically calculated mean velocities were compared successfully with PIV measurements.

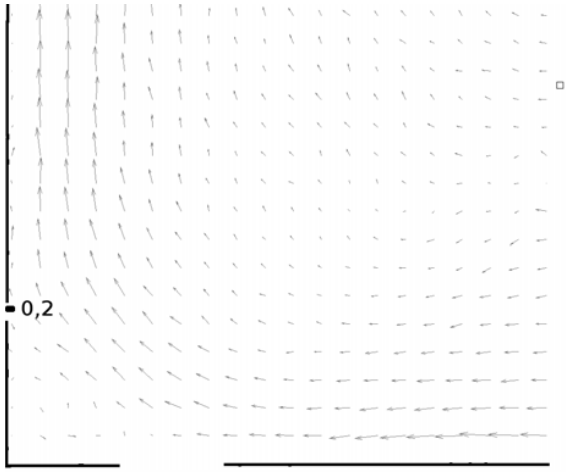

Fig. 7. The mean velocity in the slice visualized by the PIV method

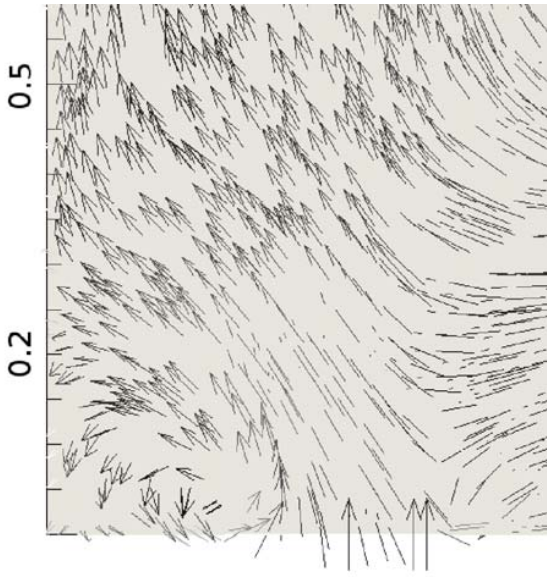

Fig. 8. Vectors of the mean velocity calculated using the laminar approach

Fig. 7 shows a mean velocity depicted by a vector field and measured by a PIV method. The heated air flow coming into the room mixes with the flow from the surrounding space and this mixture rises up along the vertical cooled wall. Later, this flow partially splits into the main flow and continues to rise up. The weaker part of this flow goes back to interact later with the heated air flow again. This separation point was identified experimentally to be approximately at the height of 0.2 m from the bottom. This value was confirmed numerically and furthermore the same flow tendencies were observed numerically, as well. The calculated results are depicted in Fig. 8, where the vectors represent the mean velocity plotted in the slice with a distance 0.15 mm of the plane symmetry.

Fig. 9 (left) illustrates a region where the air temperature is higher than 1.01 T_0. The heated air could reach the top of the room and could continually spread in various directions at the

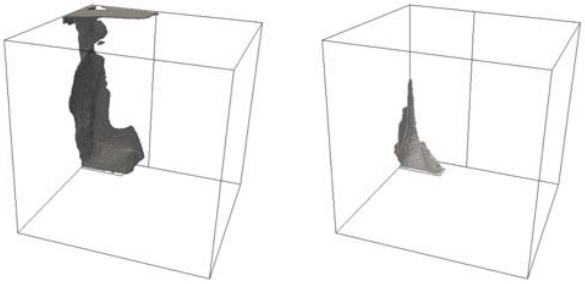

Fig. 9. Iso-surfaces of the temperature level from 1.01 T_0 up to 1.03 T_0. The wall distance is 11 mm at the surrounding temperature of T_0 (left) and with the temperature of 0.95 T_0 (right) both calculated using the laminar approach.

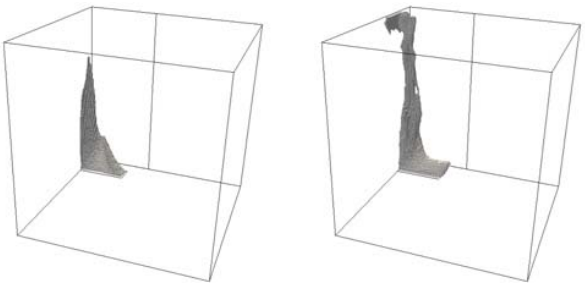

Fig. 10. Iso-surfaces of the temperature level from 1.01 T_0 up to 1.03 T_0. The wall distance is 11 mm at the surrounding temperature of T_0 calculated using the k-omega turbulence model (left) and with the wall distance of 16 mm calculated with the laminar approach.

top. Meanwhile the heated air rising to the top of the room has been influenced by the wall which has same temperature as the surroundings. Because the temperature difference between the wall and heated air was not particularly high, the heat transfer from the heated air to the wall was low. Consequently, the cooling of the air was not significant. Fig. 9 (right) shows a similar example to the previous one, however, the wall temperature was 0.95 T_0. In this case, the cooled wall had a crucial effect on the rate of cooling of the rising air. As it is in Fig. 9, the air with a temperature of more than 1.01 T_0 could not reach the top of the room because it was more intensively cooled by the vertical wall. Simultaneously, part of the heated air was deflected by the vertical wall and air was steaming directly into the room. This fact was confirmed experimentally using PIV visualization as well. As a result, the cooled wall had a significant effect on the temperature distribution vertically, however, only a maximal temperature difference of 0.05 T_0 between the surrounding temperature and wall was considered in this study.

Fig. 10 illustrates the region for the same example as in Fig. 9, but the laminar approach was replaced by turbulence modeling based on the two-equation turbulence model $k - omega$. Assuming the region with the temperature more than 1.01 T_0, this region was evidently smaller than the previous example, it is because the heated air flow was cooled more intensively. This fact was observed even if the wall distance was changed from 11 mm to 16 mm. It points out that if the turbulence model was used for turbulence prediction and accounted for the flow behavior, the heat transfer was more

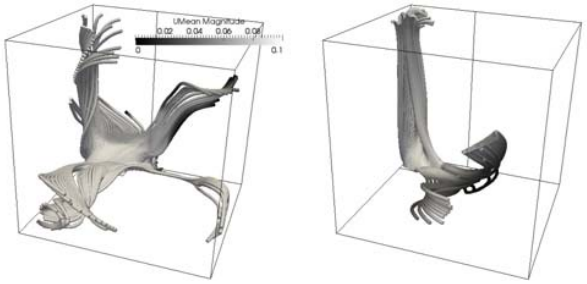

Fig. 11. Iso-surfaces of the mean velocity for wall distance of 11 mm and calculated using the laminar approach (left) and a turbulence model (right)

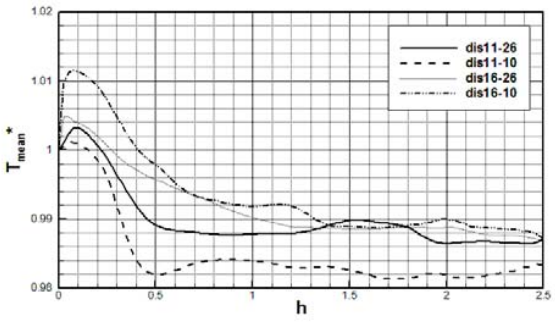

Fig. 12. Temperature distribution of the indoor air flow calculated with the laminar approach

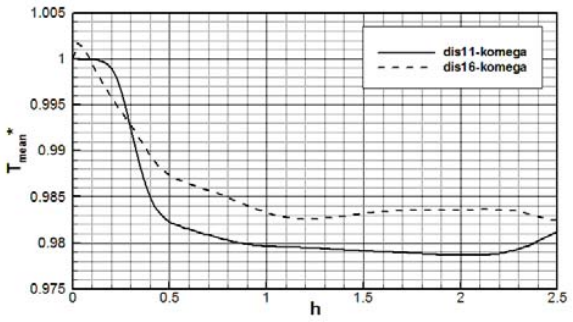

Fig. 13. Temperature distribution of the indoor air flow with the turbulence model k-omega

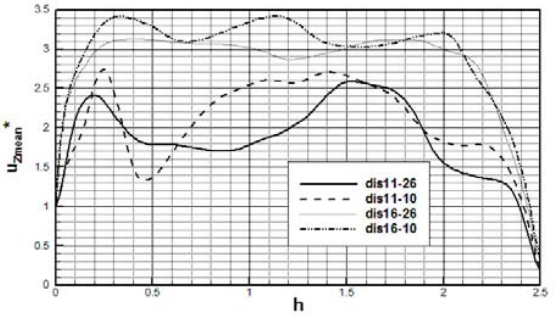

Fig. 14. Mean velocity z-component of the indoor air flow at the vertical direction calculated with a laminar approach

intensive and the air flow was cooled faster. Faster cooling of the heated air was observed if the wall distance was larger. Fig. 10 (right) represents an example where the wall distance was 16 mm and the solver was to be a laminar. Similarly, the region where the temperature was more than 1.01 T_0 was smaller in comparison to the case using 11 mm. On the other hand, this region was larger if the turbulence modeling was applied for calculations for the same wall distance.

Fig. 11 shows a trace of the flow in the room for a wall distance of 11 mm calculated using the laminar approach (left) and turbulence model (right). The air flow at the surrounding temperature was mixed with a heated air flow coming into the room from the heat exchanger located in the flow and this mixture rose up to the top of the room. Whereas this air flow was relatively uniform when calculated using a turbulence model, simulations using the laminar approach revealed a slight flow interaction with a slight rotation effect on the flow.

From a practical point of view, the important results associated with human observations of temperature are the temperature distribution in the room. Fig. 12 shows a temperature distribution in vertically from the center of the heat convector at the bottom up to the top of the room for cases with wall distances of 11 and 16 mm and with a cooled wall and an isothermal wall as the surrounding temperature. T^*_{mean} is time average temperature divided by the temperature of the hot air coming to the room from the heat exchanger at the bottom. In the case of a wall distance of 11 mm, the air was cooled faster in this position however, from the previous results depicted in Fig. 12, more heated air reached the top of the room. An explanation of this phenomenon is that the flow clings to the vertical wall and therefore, the temperature profiles evaluated directly above the heat exchanger revealed a rapid temperature decline. This temperature decline comes to be more evident if the wall temperature was lower than surrounding temperature in the room, at 0.95 T_0, respectively. In contrast when the wall distance increased to 16 mm it caused a more gradual drop of the temperature. That is because the flow did not cling to the vertical wall, but it rose up directly to the top of the room. Meanwhile this heated air flow had a strong interaction with the indoor flow and heat transfer was more intensive and the flow partially changed direction into the center of the room.

As described above, the turbulence model had a visible effect on the temperature distribution. Fig. 13 depicts temperature profiles above the heat exchanger. The temperature dropped down to 0.98 T_0 for a wall distance of 11 mm and a little less for 16 mm. Definitely, for both cases the temperature decline was evident and as mentioned before, it was a consequence of the turbulence involved into the flow simulation.

Fig. 14 shows the time average velocity component in the vertical direction $u^*_{z_{mean}}$ for the wall distance 11 mm and 16 mm and for the isothermal or cooled wall. The time average velocity $u_{z_{mean}}$ was scaled by the inlet velocity of the heated air u_{out} leaving the heat exchanger and coming into the heated room. Whereas the size of the wall distance influenced the intensity of the velocity, the wall temperature has no significant

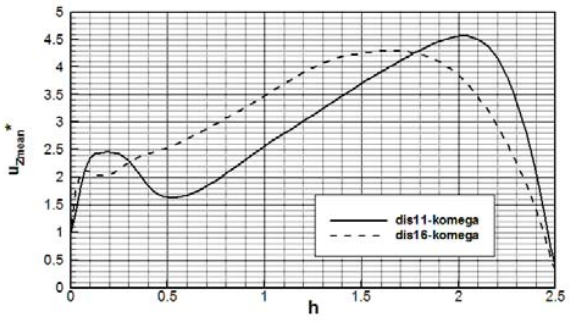

Fig. 15. Mean velocity z-component of the indoor air flow at the vertical direction calculated with a laminar approach

effect. The decline of the velocity in the z-direction was due to changes of the air flow orientation. As described above, at a wall distance of 11 mm, the air flow clung to the vertical wall and, therefore, the lower intensity of the velocity for 11 mm wall distance was found.The maximal level of the z-component of the mean velocity was approximately from 2 u_{out} to 2.5 u_{out}. For a wall distance of 16 mm, the velocity level was from 3 u_{out} to 3.5 u_{out}. Fig. 15 indicates the velocity profile of the z-component of the mean velocity calculated using the turbulence model. The velocity increased gradually up to 2 m from the bottom and then it declined due to the effect of the wall type boundary condition. The peak of the velocity was $4.2u_{out}$ for the wall distance 16 mm and even $4.5u_{out}$ for the wall distance of 11 mm, respectively.

V. Conclusion

The indoor air flow simulation was studied numerically using the computational code OpenFOAM. The size and shape of the computational domain corresponding to the real lab and boundary conditions were determined from hot wire measurements. Results obtained numerically were successfully compared with PIV measurements. The cooled wall had a significant effect on the flow behavior. In the case of the low wall temperature, the flow changed orientation and streamed into the room and less to the top of the room. In both cases, the flow asymmetry detected was caused by the stronger cross flow resulting from the geometrical asymmetry. The temperature and velocity profiles were influenced strongly by the turbulence model. Validation using experiments confirmed that the laminar flow approach was suitable for such a problem and it was because of the lower Reynolds number. If the Reynolds number would be higher, then turbulence modeling starts to be more relevant. In the future, the indoor air flow simulation will be performed on the smoother computational mesh and the influence of the Reynolds number and temperature will be examined.

Acknowledgment

This work was financially supported from the project of the Technology Agency of the Czech Republic under no. TA01020231.

References

[1] M. Schatzmann and A. J. Policastro, Effects of the Boussinesq approximation on the Results of Strongly-Buoyant Plume Calculations, *Journal of climate and applied meteorology Vol. 23* (1984), pp. 117-123
[2] M. Samdip, On the Use of the fully compressible Navier-Stokes Equations for the Steady-State Solution of Natural Convection Problem in closed Cavities, *Journal of Heat Transfer Vol. 129* (2007), pp. 387-390
[3] J. H. Ferziger and M. Peric, Computational Methods for Fluid Dynamics, *3A Practical Guide.,Springer-Verlag* (2002), pp. 14-15
[4] M. Raffel, C. Willert, S. Wereley and J. Kompenhans, Particle Image Velocimetry, *3rd revised, Springer-Verlag* (2007)
[5] R. J. Adrian, Particle-imaging techniques for experimental fluid mechanics, *Annual Review of Fluid Mechanics 23 (1)* (1991), pp. 261-304
[6] K. Frana, An Enhance of the Energy Effectiveness of the Convectors Used for Heating or Cooling, (2012), pp.
[7] J. D. Posner, C. R. Buchanan and D. Dunn-Rankin, Meassurement and prediction of indoor air flow in a model room, *Energy and Buildings 35* (2003), pp. 515-526
[8] R. Yousaf, D. Wood, M. Cook, T. Yang, S. Hodder, D. Loveday and M. Passmore, CFD and PIV based investigation of indoor air flows dominated by buoyancy generated by human occupancy and equipment, *Proceeding of Building Simulation* (2011), pp. 1465-1472
[9] W. Zhang and Q. Chen, Large eddy simulation of indoor airflow with a filtered dynamic subgrid scale model, *International Journal of Heat and Mass Transfer 43* (2000), pp. 3219-3231
[10] S. L. Sinha, R. C. Arora, S. Roy, Numerical simulation of two-dimensional room air flow with and without buoyancy, *Energy and Buildings 32* (2000), pp. 121-129
[11] D. C. Wilcox, Turbulence modelling for CFD, 2nd edition, *DCW Industries, Inc., La Canada CA* (1998)